

## Pulse Height Distribution and Radiation Tolerance of CVD Diamond Detectors

### *The RD42 Collaboration:*

W. Adam<sup>1</sup>, E. Berdermann<sup>3</sup>, P. Bergonzo<sup>4</sup>, G. Bertuccio<sup>5</sup>, F. Bogani<sup>6</sup>, E. Borchi<sup>7</sup>, A. Brambilla<sup>4</sup>, M. Bruzzi<sup>7</sup>, C. Colledani<sup>8</sup>, J. Conway<sup>9</sup>, P. Dangelo<sup>10</sup>, W. Dabrowski<sup>11</sup>, P. Delpierre<sup>12</sup>, A. Deneuve<sup>13</sup>, W. Dulinski<sup>8</sup>, B. van Eijk<sup>14</sup>, A. Fallou<sup>12</sup>, F. Fizzotti<sup>15</sup>, F. Foulon<sup>4</sup>, M. Friedl<sup>1</sup>, K.K. Gan<sup>16</sup>, E. Gheeraert<sup>13</sup>, E. Grigoriev<sup>17</sup>, G. Hallewell<sup>12</sup>, S. Han<sup>16</sup>, F. Hartjes<sup>14</sup>◇, J. Hrubec<sup>1</sup>, D. Husson<sup>8</sup>, H. Kagan<sup>16</sup>, D. Kania<sup>16</sup>, J. Kaplon<sup>17</sup>, C. Karl<sup>18</sup>, R. Kass<sup>16</sup>, M. Krammer<sup>1</sup>, A. Logiudice<sup>15</sup>, R. Lu<sup>15</sup>, C. Manfredotti<sup>15</sup>, D. Meier<sup>17</sup>, M. Mishina<sup>19</sup>, L. Moroni<sup>10</sup>, A. Oh<sup>18</sup>, L.S. Pan<sup>16</sup>, M. Pernicka<sup>1</sup>, A. Peitz<sup>9</sup>, S. Pirollo<sup>7</sup>, P. Polesello<sup>15</sup>, M. Procaro<sup>20</sup>, J.L. Riestler<sup>7</sup>, S. Roe<sup>17</sup>, L. Rousseau<sup>4</sup>, A. Rudge<sup>17</sup>, J. Russ<sup>20</sup>, S. Sala<sup>10</sup>, M. Sampietro<sup>5</sup>, S. Schnetzer<sup>9</sup>, S. Sciortino<sup>7</sup>, H. Stelzer<sup>3</sup>, R. Stone<sup>9</sup>, B. Suter<sup>20</sup>, R.J. Tapper<sup>23</sup>, R. Tesarek<sup>9</sup>, M. Trawick<sup>16</sup>, W. Trischuk<sup>21</sup>, D. Tromson<sup>4</sup>, E. Vittone<sup>15</sup>, A.M. Walsh<sup>9</sup>, R. Wedenig<sup>1</sup>, P. Weilhammer<sup>17</sup>, C. White<sup>22</sup>, W. Zeuner<sup>18</sup>, M. Zoeller<sup>16</sup>.

### *Other contributors:*

A. Fenyvesi<sup>24</sup>, J. Molnar<sup>24</sup>, D. Sohler<sup>24</sup>.

<sup>1</sup> Institut für Hochenergiephysik der Österreichischen Akademie der Wissenschaften, A-1050 Vienna, Austria

<sup>3</sup> GSI, Darmstadt, Germany

<sup>4</sup> LETI (CEA-Technologies Avancees) DEIN/SPE - CEA Saclay, 91191 Gif-Sur-Yvette, France

<sup>5</sup> Ploytechnico of Milano, Italy

<sup>6</sup> LENS, Florence, Italy

<sup>7</sup> University of Florence, Florence, Italy

<sup>8</sup> LEPSI, IN2P3/CNRS-ULP, Strasbourg 67037, France

<sup>9</sup> Rutgers University, Piscataway, NJ 08855, U.S.A.

<sup>10</sup> INFN Milano, Italy

<sup>11</sup> Faculty of Physics and Nuclear Techniques, UMM, Cracow, Poland

<sup>12</sup> CPPM, Marseille 13288, France

<sup>13</sup> LEPES, Grenoble, France

<sup>14</sup> NIKHEF, Amsterdam, Netherlands

<sup>15</sup> Univerity of Torino, Italy

<sup>16</sup> The Ohio State University, Columbus, OH 43210, U.S.A.

<sup>17</sup> CERN, CH-1211, Geneva 23, Switzerland

<sup>18</sup> II.Inst. für Exp. Physik, Hamburg, Germany

<sup>19</sup> FNAL, Batavia, U.S.A.

<sup>20</sup> Carnegie-Mellon University, Pittsburgh, U.S.A.

<sup>21</sup> University of Toronto, Toronto, ON M5S 1A7, Canada

<sup>22</sup> Illinois Institute of Technology, Chicago, IL 60616, U.S.A.

<sup>23</sup> Bristol University, Bristol BS8 1TL, U.K.

<sup>24</sup> ATOMKI, Debrecen, Hungary. work supported by Hungarian Research Fund (T026184)

---

◇ representing the RD42 collaboration (F.Hartjes@nikhef.nl)

## ABSTRACT

The paper reviews measurements of the radiation tolerance of CVD diamond for irradiation with 24 GeV/c protons, 300 MeV/c pions and 1 MeV neutrons. For proton and neutron irradiation, the measured charge signal spectrum is compared with the spectrum calculated by a model.

Irradiation by particles causes radiation damage leading to a decrease of the charge signal. However, both the measurements and the outcome from the model show that for tracker applications this drawback is at least partly counterbalanced by a narrowing of the distribution curve of the charge signal. In addition, we observed after proton irradiation at the charge signal spectrum a decrease of the number of small signals. As a result, the efficiency of a CVD diamond tracker is less affected by irradiation than the mean charge signal.

## 1 INTRODUCTION

Since 1990, there have been very significant improvements in the performance of particle detectors using CVD diamond. The charge collection distance (CCD), being the figure of merit for diamond particle detectors, has shown an increase from a few micrometers to more than 200  $\mu\text{m}$ , corresponding to a mean signal of 7200 electrons, nowadays [1]. Having a smaller charge signal than for silicon, detectors made from CVD diamond have the advantage of a low electrode capacitance, low leakage current and a high radiation tolerance. For this paper, we concentrate especially on the application of CVD diamond as a tracking detector for highly energetic charged particles.

The charge collection distance depends on the presence of charge carrier traps[2]. Once a deep level trap has captured a charge carrier the trap is permanently passivated, a process called 'pumping'. CVD diamond remains for a long period (months) in the pumped state if kept in the dark and at room temperature. To pump CVD diamond a fluence of the order of  $10^{10}$  minimum ionising particles (m.i.p.s) per  $\text{cm}^2$  is generally sufficient. In contrast to this, shallow traps remain active at room temperature since they capture the charge carrier only for a short period.

Most CVD diamond has a polycrystalline structure with an average crystal size of the order of 1/7 of the thickness on the growth side [4]. On the substrate side the crystal size is only a few micrometers. The CVD diamond that is presently in use by RD42 appears to have a broad distribution of the charge

collection distance across the different crystals [4]. The result is a widening of the distribution of the charge signal from the whole substrate. The broadening of the charge signal distribution from m.i.p.s has been observed to decrease after irradiation.

The radiation damage to CVD diamond by particles mainly consists of interstitials and vacancies, acting as charge traps. Assuming this effect to occur by the same amount for all crystals, the result of irradiation of CVD diamond will be an equal increase of the trap density for all crystals leading to a better uniformity. It also implies a faster degradation due to radiation for diamond with initially high charge signal, i.e. a low trap density, compared to diamond having a poor charge collection. Apart from radiation damage we have observed for protons after  $10^{15} \text{ cm}^{-2}$  an increase of the signals at the low side of the charge signal spectrum.

For an individual diamond crystal the charge signal distribution has the shape of a Landau curve where the average signal depends on the density of the traps. Accordingly, for the signal from an extended area of polycrystalline CVD diamond we get a broader distribution consisting of the convolution of the Landau curves from a multitude of crystals.

To be able to predict the radiation effects on CVD diamond, we have derived a model incorporating radiation damage and a possible decrease of the number of small signals after irradiation. The model yields the distribution curve of the charge signal as a function of the particle fluence.

In this paper, we characterise CVD diamond not only by the charge collection distance but also by the threshold above which 90% of the events fall.

## 2 EXPERIMENTAL CONDITIONS

### 2.1 Irradiation

For the irradiation measurements, samples were used having a circular electrode of 3 - 7 mm diameter on the front and backside to enable characterisation. The proton irradiation was performed at CERN in the PS beam using 24 GeV/c protons [3, 4]. The neutron irradiations were performed at the Atomki cyclotron in Debrecen, Hungary, the pion irradiations at PSI using 300 MeV/c pions [5].

### 2.2 Characterisation

Before and after the irradiation steps, the sample was measured using a collimated  $^{90}\text{Sr}$  source. A trigger detector (silicon diode or scintillator) was located downstream. In this way events having an energy loss close to the minimum were selected. The charge signal from the sample was amplified by a low noise amplifier (200-350 NEC) having a shaping time of a few microseconds and recorded by a DAQ system. All samples were pumped before characterisation. Normally between 800 and 5000 events were recorded for each charge spectrum.

The characterisation was done at a bias field of + 1 and - 1 V/ $\mu\text{m}$ . For the proton and neutron spectra a fit was made using an empirical Landau expression [6]

$$L(Q, p_1, b) = \frac{a}{b} e^{-\frac{1}{2}(G+e^{-G})} \quad (1)$$

where  $G(Q, p_1, b) = \frac{Q - p_1}{b}$ ,  $a (\approx 2.506)$  is the normalisation factor quantified by  $\int_{-\infty}^{\infty} L(Q) dQ = 1$ ,  $Q$  is the charge signal,  $p_1$  is

the most probable value and  $b$  is the variance factor ( $b \approx \text{RMS}_{\text{Landau}} / 2.221$ ).

The Landau curve was convoluted with a Gaussian to account for the electronic noise of the preamp. For most distributions, a pedestal peak was present originating from background triggers. Often the pedestal peak has been useful in determining the zero reference of the spectrum.

## 3 MODEL DESCRIBING THE IRRADIATION EFFECTS

### 3.1 Modelling the distribution function

To derive an expression for the charge signal distribution as a function of the fluence, we start by describing the signal distribution before irradiation. The derivation is found in more detail in [7].

For a single diamond crystal, we assume the response to be a Landau function (L) that we approximate by (1). As a next step we introduce a function (F) describing the distribution of the average charge signal across the substrate. Since F is directly linked to the distribution of the trap concentration across the substrate, F should be asymmetric at wide distributions to avoid negative trap concentrations. Therefore, we take the most likely function, a Gaussian of the logarithm of the average crystal\* charge signal ( $\bar{Q}$ ), as an expression for the broadening of the distribution curve by the polycrystalline structure

$$F(\bar{Q}) \propto \frac{e^{-\frac{\ln(\bar{Q})^2}{2\sigma^2}}}{\sigma\sqrt{2\pi}} \quad (2)$$

where  $\sigma$  is the width of the Gaussian.

Accordingly we get for the total distribution function (H) of the charge signal (Q) the convolution of F and L:

---

\* For the derivation in Ch. 3 the term 'crystal' stands for an infinitesimal small area on the substrate. The term is only used for ease of speaking.

$$H(Q) = \int F(q) \cdot L\{Q, q'(q), b(q)\} dq, \quad (3)$$

where  $b(q) = b_0 \cdot q'(q)$ ,  $b_0$  being the relative variance factor of the single crystal Landau,  $q'(q) = q - \alpha \cdot b$  and  $\alpha \approx 1.27$ . The value for  $\alpha$  has been chosen such that the mean value of  $H$  ( $\langle H \rangle$ ) equals the mean value of  $F$  ( $\langle F \rangle$ ).

### 3.2 Radiation dependent distribution

In the model we consider two different effects from irradiation:

1. Creation of new traps in the bulk.
2. Increase of the small charge signals after irradiation.

For simplicity we assume in the following equal parameter values for electrons and holes. We define  $\lambda$  as the mean path of an electron/hole pair before trapping. From literature [8] the dependence of  $\lambda$  on the fluence  $\phi$  is known as

$$\frac{1}{\lambda(\phi)} = \frac{1}{\lambda(0)} + g \cdot \phi \quad (4)$$

where  $g$  is the radiation damage constant. Adding trap passivation like pumping to describe a possible small signal increase brings us to

$$\frac{1}{\lambda(\phi)} = \frac{1 - \delta + \delta \cdot e^{-\gamma\phi}}{\lambda(0)} + g \cdot \phi \quad (5)$$

where  $\delta$  is the fraction of the traps that potentially can be passivated and  $\gamma$  is the passivation constant. There is a direct relation [2] in the crystal between  $\bar{Q}$  and  $\lambda$ :

$$\bar{Q} = \rho \cdot \lambda \quad (6)$$

for  $\lambda \ll D$

where  $\rho$  is the density of electron/hole pairs for a m.i.p. along the track ( $\rho = 36$  e/h pairs / $\mu\text{m}$ ) and  $D$  is the detector thickness. Note

that  $\lambda$  is equal to the charge collection distance as long as the condition in (6) is true.

To convert the distribution function (3) into a radiation dependent expression we assume that only  $F$  is affected by irradiation. Accordingly, we calculate using (5) and (6) for each value  $q$  in the distribution of the irradiated sample after fluence  $\phi$  the value  $q_0$  in the spectrum of the non-irradiated sample

$$q_0(q, \phi) = \frac{1 - \delta + \delta \cdot e^{-\gamma\phi}}{1/q - g \cdot \phi / \rho} \quad (7)$$

$$\text{if } 0 < q < \frac{\rho}{g \cdot \phi}.$$

However, to get the correct number of events at  $q_0$  we have to multiply the number of events at  $q$  by  $\frac{dq_0(q)}{dq}$ .

As a result we get for the radiation dependent distribution function

$$\begin{aligned} H(Q, \phi) &= \\ &= \int F\{q_0(q)\} \frac{dq_0(q)}{dq} L\{Q, q'(q), b(q)\} dq \quad (8) \end{aligned}$$

## 4 RESULTS OF THE IRRADIATIONS

### 4.1 Proton irradiation

Three dot samples that originated from substrate CD-S12 received at first a fluence of  $0.9 \cdot 10^{15} \text{ cm}^{-2}$ . Subsequently, they underwent a second irradiation at 5.0, 4.1 and  $3.2 \cdot 10^{15} \text{ cm}^{-2}$  for P1, P2 and P3 respectively. The leakage current between the spills did not increase during irradiation. Also the particle-induced current of approximately 1.5  $\mu\text{A}$  remained constant. Details about the irradiation and characterisation are found in ref. [3].

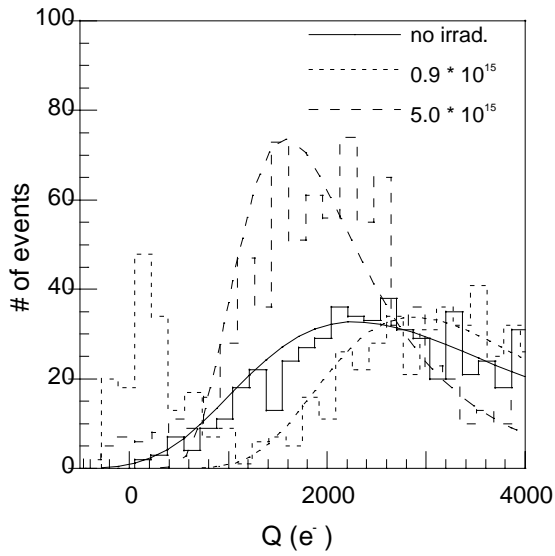


Fig. 1. Distribution of the charge signal ( $Q$ ) of CD-S12 P1 for three different levels of proton irradiation.

Fig 1 shows the measured charge signal distribution for P1 at three different levels of irradiation together with the fitted Landau curves. The zero reference of the measurements was obtained from the average signal of measurements done without bias voltage. The figure shows that there is a shift of the rising edge of the Landau curve at  $0.9 \cdot 10^{15} \text{ cm}^{-2}$ . On the other hand, at  $5.0 \cdot 10^{15} \text{ cm}^{-2}$  radiation damage dominates. The decrease in the number of small signals raises the threshold above which 90% of the signals fall as shown in fig 2. There is no degradation of the efficiency until  $3 \cdot 10^{15} \text{ cm}^{-2}$  protons.

For the calculation of the model prediction in fig. 1 by expression (8), the model parameters were chosen such that the best correspondence between the measured and the calculated distribution was obtained [7]. Accordingly we obtained for the radiation damage constant  $g = 2.8 \pm 0.4 \cdot 10^{-14} \text{ cm}$  and for the passivation constant  $\gamma = 7.2 \pm 0.5 \cdot 10^{-16} \text{ cm}^2$ . The passivation fraction had been set to  $\delta = 75\%$ . The uniformity factor  $K$  for CD-S12 was found as  $K = 1.56 \pm 0.10$  ( $K = \exp(\sigma)$ ).  $b_0$  has been set at 0.16, a value corresponding to 36% rms. We derived this number from the

width of the distribution after high fluences where the Landau width dominates. The charge collection distance was  $72 \pm 6 \mu\text{m}$ .

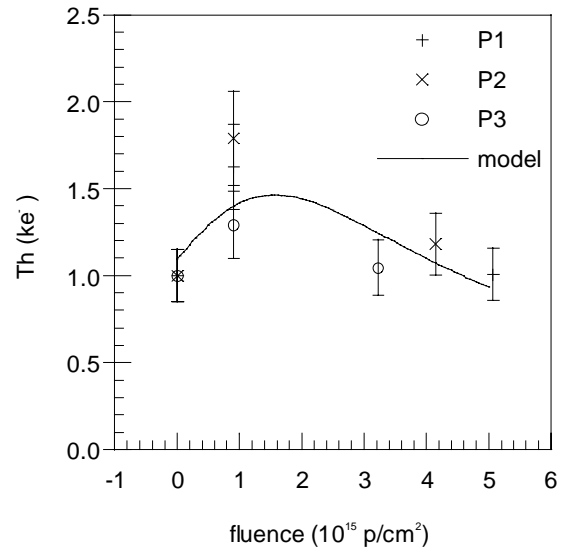


Fig. 2. Measured threshold (Th) above which 90% of the events fall, as a function of the received proton fluence for CD-S12 P1, P2 and P3.

## 4.2 Neutron irradiations

Two samples from UT-S1, P14 and P16, having a charge collection distance around  $120 \mu\text{m}$  were irradiated at Atomki, by 3 different fluences up to  $2.0 \cdot 10^{15} \text{ cm}^{-2}$ . The result is shown in fig. 3.

The degradation of the charge signal is smaller than measured earlier at samples irradiated at ISIS on RAL, UK [4, 9]. The different result could be caused by the different material properties (UT-S1 is at least 2 years more recent than the material used for the ISIS measurements) or by the different energy spectrum. ISIS has an energy spectrum of 'fast' neutrons peaking around 1 MeV [4] while the energy spectrum at Atomki has a continuous decrease above 0.1 MeV by a factor of 12 per decade followed by a sharp cut-off at 15 MeV[10, 11].

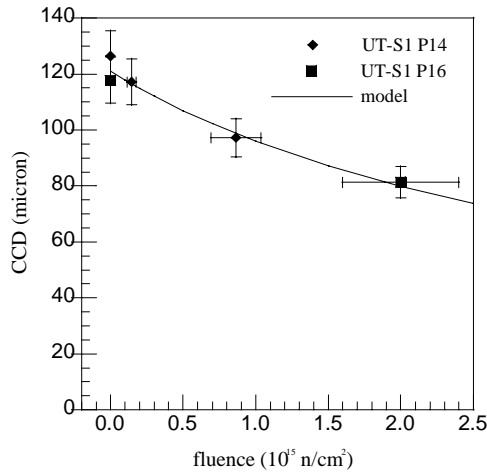


Fig. 3. Measured charge collection distance (CCD) as a function of the applied neutron fluence.

The measured distribution curves before and after irradiation were fitted to the distribution (8) of the model. Typical examples are shown in fig. 4 and fig 5.

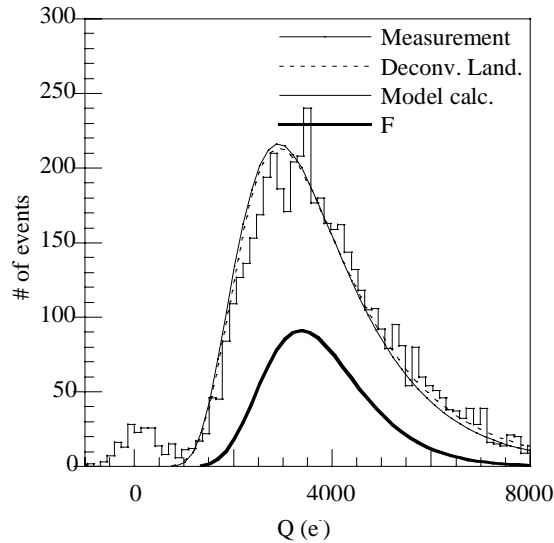


Fig. 4. Distribution of the charge signal of UT-S1-P16 at -1 V/μm before irradiation.

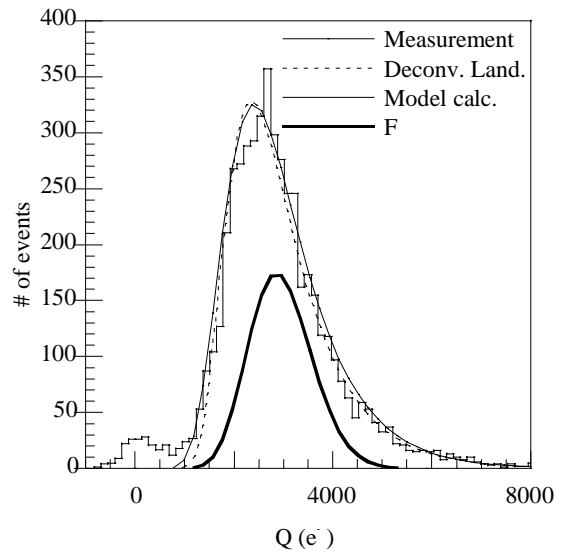


Fig. 5. Distribution of the charge signal (Q) of UT-S1-P16 at -1 V/μm after a neutron irradiation of  $2.0 \pm 0.4 \cdot 10^{15} \text{ cm}^{-2}$

The histograms have been fitted by a Landau convoluted with Gaussian electronic noise ( $\sigma = 330 e^-$ ). Since the model only deals with the pure diamond signal with exclusion of electronic noise, only the deconvoluted Landau (dotted line) is plotted as a comparison. Convolution with noise results into a minor increase of the most probable value like is illustrated by the histograms of the measured data. The correspondence between the deconvoluted Landau from the measurements and the predicted curve from the model (thin solid line) is good in the non-irradiated case and reasonable for the irradiated case. To calculate the distribution expression (4) having no passivation effect was applied.

A much better fit for the model distribution in fig. 5 was obtained using (5) instead of (4) with a few passivation added. However, the other spectra did not give sufficient evidence to justify this.

The plots also show the calculated uniformity curve F. Before irradiation, the curve has the asymmetric and Landau-like shape that is given by the logarithmic Gaussian function. After irradiation, the tail

at the higher amplitudes has been greatly reduced while the region of the low amplitudes underwent less change. Indeed, diamond crystals that have a low concentration of traps, giving rise to high charge signals, are more affected by the additional radiation-induced traps. This phenomenon has its impact on the efficiency. After  $2 \cdot 10^{15} \text{ cm}^{-2}$ , the threshold above which 90% of the events fall has been only reduced from 2200 to 1600  $e^-$  (25 %), while the mean charge signal has decreased by 31%.

Fitting the model parameters to the measured spectra yielded a radiation damage constant  $g = 2.0 \pm 0.5 \cdot 10^{-14} \text{ cm}$ . The uniformity factor for UT-S1 was  $K = 1.34 \pm 0.03$ . The width  $b_0$  of the single crystal Landau has been set at 0.14 (31% rms.). The charge collection distance was  $127 \pm 2$  and  $118 \pm 2 \text{ }\mu\text{m}$  for P14 and P16 respectively. The model prediction plotted in fig. 3 is the mean of (8) averaged over P14 and P16. The curve shows a good agreement with the measurements.

The spectra have good statistics (5000 events per spectrum). Therefore, in this case the correct value for the variance factor  $b_0$  of the single crystal Landau was easily found by comparing the tail of the predicted curve with the measurement. If  $b_0$  is not correct then the tail of the predicted curve does not fit, a phenomenon that cannot be compensated by modifying the width of the Gaussian distribution. The smaller value for  $b_0$  compared to the one found from the proton data may be caused by the rather poor statistics of the proton characterisation.

### 4.3 Pion irradiation

Fig. 6 shows the results of various pion irradiations performed at PSI. In the picture a common decrease of the charge collection distance is clearly visible. The plot also shows the tendency for a faster degradation at higher values of the charge collection distance as expected from the model.

Presently, the measurements are being repeated using recently produced material.

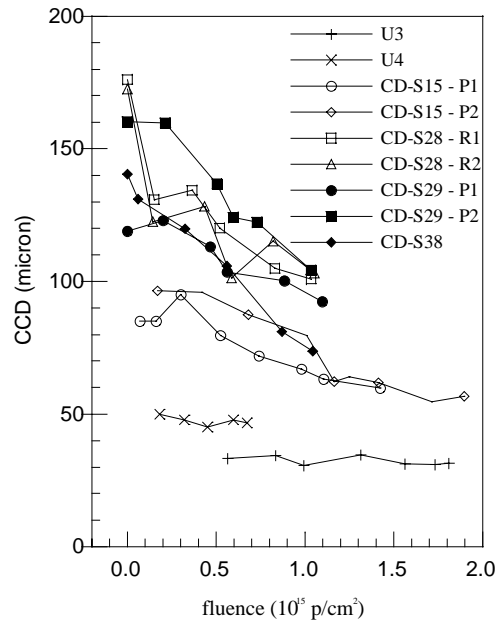


Fig. 6. Charge collection distance (CCD) as a function of the pion fluence.

### CONCLUSIONS

The measurements shown in this paper demonstrate that CVD diamond is roughly an order of magnitude more radiation hard than silicon. Still bulk damage is the main effect of radiation by particles reducing the charge signal. On the other hand, the paper also shows that irradiation leads to improvement of the uniformity. Therefore we may state that for proton, neutron and pion irradiation not much degradation of the tracker performance is expected after a fluence of the order of  $10^{15} \text{ cm}^{-2}$ . At this level the efficiency has not much changed while the uniformity has significantly improved. The spectra measured after proton irradiation show a clear decrease of the number of small charge signals.

The results also demonstrate the progress in the production of more uniform diamond. The width of the uniformity distribution for substrate UT-S1, delivered June 1998, is a factor of 1.5 less than for substrate CD-S12, delivered March 1996.

## REFERENCES

---

- 1 S. Schnetzer et al. (RD42 Collaboration), "Tracking with CVD Diamond Radiation Sensors at High Luminosity Colliders", IEEE Transactions on Nuclear Science, Vol. 46(1999), 193-200.
- 2 S. Zhao, "Characterisation of the Electrical Properties of Polycrystalline Diamond Films", PhD thesis Ohio State University (1994).
- 3 D.Meier et al. (RD42 Collaboration), "Proton Irradiation of CVD Diamond Detectors for High Luminosity Experiments at the LHC", NIM A 426 (1999) 173.
- 4 D.Meier, "CVD Diamond Sensors for Particle Detection and Tracking", PhD thesis Univ. of Heidelberg, Germany, (1999).
- 5 C. Bauer et al. (RD42-Collaboration). "Pion Irradiation Studies of CVD Diamond Detectors". Pre-print CERN-PPE/95-173, (1995).
- 6 J.E. Moyal, "Theory of Ionization Fluctuations", Philosophical Magazine 46 (1955), 263-280.
- 7 F. Hartjes et al. (RD42 Collaboration), "Parameterisation of radiation effects on CVD diamond for proton irradiation". Nucl. Phys. B (Proc. Suppl.) 78 (1999) 675.
- 8 E. Borchini and M. Bruzzi, "Radiation Damage in Silicon Detectors". La Rivista del Nuovo Cimento 17 (1994) 11, expression (6.2) where  $\lambda$  has been substituted by  $\tau$  (carrier lifetime).
- 9 W. R. Wedenig, "Development of Superconducting NbN Microstrip Detectors and CVD Diamond Detectors for Particle Detection and Tracking" PhD thesis, Technical University of Vienna, Austria (1999).
- 10 M.A. Lone et al., "Thick target neutron yield and spectral distributions from the Li-7(p,n), Li-7(d,n), Be-9(p, n), Be-9(d,n) reactions", NIM 143 (1977) 331-344.
- 11 A. Fenyvesi et al., " Package irradiation studies", CERN/RD-16 / FERMI Collaboration Note 14 (January 1993).